Available online at www.sciencedirect.com

ScienceDirect

IFAC PapersOnline CONFERENCE PAPER ARCHIVE

IFAC PapersOnLine 58-21 (2024) 162–167

A Two-Dimensional State-Space Model for Metal Hydride Storage Tanks and Parameter Sensitivity Analysis ⋆

Mingrui Chen * **Carles Batlle** ** **Ramon Costa-Castelló** *
Jing Na ***,****

* *Institut de Robòtica i Informàtica Industrial, CSIC-UPC. C/ Llorens i Artigas 4-6, 08028 Barcelona, Spain (e-mail: chenmingrui2018@gmail.com; ramon.costa@upc.edu).*
** *Departament de Matemàtiques, Institut d'Organització i Control, EPSEVG, UPC, 08800 Vilanova i la Geltru, Spain (e-mail: carles.batlle@upc.edu)*
*** *Faculty of Mechanical and Electrical Engineering, Kunming University of Science and Technology, Kunming, 650500, PR China (e-mail: najing25@163.com)*
**** *Yunnan Key Laboratory of Intelligent Control and Application, Kunming, 650500, PR China*

Abstract: Modeling of metal hydride storage tanks remains a challenging issue. In most of the literature, the charge and discharge of metal hydride storage tanks are controlled by the hydrogen flow rate. However, the case of controlling the charge and discharge of metal hydride tanks by pipe pressure has rarely been reported in the literature. Aiming at this problem, this work presents a two-dimensional state-space model that takes the pipe pressure as the system input and assumes that the tank temperature can be measured. Then, the First-order Trajectory Sensitivity Analysis method is used to analyze the parameter sensitivity of several selected unknown parameters. The results of the sensitivity analysis indicate that six parameters: entropy change for desorption ΔS_d, enthalpy change for desorption ΔH_d, activation energy for absorption E_a, activation energy for desorption E_d, plateau flatness coefficient φ and plateau hysteresis coefficient β have higher sensitivity to the model state.

Keywords: Metal hydride tanks, State-space model, Sensitivity analysis

1. INTRODUCTION

Solid-state hydrogen storage is one of the important hydrogen storage technologies (Tarhan and Çil (2021)). Metal hydride (MH) hydrogen storage tanks have received wide attention as a container for solid-state hydrogen storage. To study the internal states of the MH tank and further estimate the state of charge (SOC) of the tank, a reasonable model for the MH tank is required.

Many researchers have studied the reaction kinetics model of the MH tank. Førde et al. (2007) proposed a kinetic expression for AB_5-type alloy and they designed an experiment to verify the validity of the proposed kinetics model. The sorption kinetics of AB_2-type alloy were studied and modeled by Hariyadi et al. (2022). They found that the reaction kinetics of AB_2-type alloy follows the Johnson-Mehl-Avrami-Kolmogorov (JMAK) model and obtained the value of the exponent for both absorption and desorption. The expressions of the kinetics mentioned in the above two literature are commonly used for analysis. Nasrallah and Jemni (1997) used an expression containing terms relating to the density of the MH to describe the reaction rate, and the equation they proposed was more convenient to use in the modeling. The equilibrium pressure of MH tanks is usually calculated using the Van't Hoff equation. However, the standard Van't Hoff equation only can be used for fixed hydrogen-to-metal atomic ratios (H/M) and the pressure-composition-temperature (PCT) curve of metal alloy has hysteresis. Thus, Jemni and Nasrallah (1995a) used a 5-order polynomial to calculate the equilibrium pressure and Nishizaki et al. (1983) added several hysteresis and slope constants in the equilibrium pressure equation.

Parameters in the model may have different effects on model states, so it is necessary to perform sensitivity analysis on different model parameters to determine the magnitude of the effect of each parameter on model states. Christopher Frey and Patil (2002) classified sensitivity analysis methods into three main categories: mathematical method, statistical method and graphical method. They selected ten different sensitivity analysis methods and

⋆ This work is part of the Project MAFALDA (PID2021-126001OB-C31 funded by MCIN/ AEI /10.13039/501100011033 and by "ERDF A way of making Europe"), the Project MASHED (TED2021-129927B-I00 funded by MCIN/AEI /10.13039/501100011033 and by the "European Union NextGenerationEU/PRTR"). This work is partially supported by Chinese Scholarship Council (CSC) under grant (202208530009).

10.1016/j.ifacol.2024.10.167

analyzed them in comparison with some criteria. Choi et al. (1999) used Multi-Parametric Sensitivity Analysis (MPSA) to analyze the relative importance of factors influencing the natural attenuation of mining contaminants. Similarly, Correa et al. (2005) used MPSA to analyze parameter sensitivity in the PEMFC model. MPSA requires the determination of nominal parameters and a large number of Monte Carlo simulations are needed to perform the analysis, which can be time-consuming when the number of parameters is large. Benchluch and Chow (1993) used the trajectory sensitivity technique to analyze the parameter sensitivity of nonlinear excitation system models. This method does not require linearization of the model and can be used to obtain the sensitivity directly from the nonlinear model. The same approach was used in (Kong et al. (2015)) to analyze the effect of parameter variations on the displacement step response of the system for nine different operating conditions of the valve-controlled cylinder. For MH tanks, Suárez et al. (2022) investigated the sensitivity of three parameters of MH tanks that change significantly from healthy to degraded state. Xiao et al. (2023) proposed a new multi-parameter sensitivity analysis method, which is based on Latin hypercube sampling and the rank correlation method, then they investigated the sensitivity ranking of 10 parameters in the PCT curve model according to the new method.

In most mathematical models of the MH tank, the mass balance equation for hydrogenation reactions usually contains a mass flow rate term which can be calculated by the flow rate data from flow meters. When the charging and discharging process of the MH tank are tuned by pipe pressure, the mass balance equation including the mass flow rate cannot be directly applied and this scenario is rarely considered in most literature. Concerning this fact, this work proposes a two-dimensional state-space model of the MH tank where a simple pipe model is introduced to calculate the mass flow rate using the pressure difference between the tank and pipe. Besides, to investigate the sensitivity of the model parameters, a trajectory sensitivity analysis method is used in this work.

This paper is organized as follows: Section 2 describes the general structure of the MH tank. Section 3 presents the physical model and two-dimensional state-space model. The sensitivity analysis of the proposed model is introduced in Section 4, and some conclusions are drawn in Section 5.

2. SYSTEM DESCRIPTION OF THE MH TANK

Figure 1 shows the schematic of the MH tank charging process. Hydrogen enters the tank through the outlet. As the pressure increases, the hydrogen starts to react with the metal alloy inside the tank when the tank pressure is larger than the absorption equilibrium pressure and this process is known as hydrogen absorption. The desorption happens when the tank pressure is lower than the desorption equilibrium pressure. The chemical equation of the sorption (absorption and desorption) process is (Afzal et al. (2017))

$$\mathrm{M} + \frac{\mathrm{x}}{2}\mathrm{H_2} \underset{\text{desorption}}{\overset{\text{absorption}}{\leftrightarrow}} \mathrm{MH_x} + \Delta\mathrm{H}, \tag{1}$$

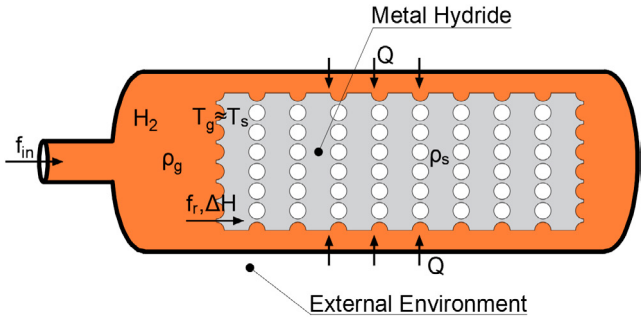

Fig. 1. Schematic of the MH tank (the process of charge).

where M is the metal alloy, $\mathrm{MH_x}$ is the MH and ΔH is the heat of reaction.

The absorption process of hydrogen releases heat while the desorption process absorbs heat. When leakage occurs in the MH tank, the pressure inside the tank decreases, allowing hydrogen to be released from the MH. This process absorbs a large amount of heat, so the temperature of the tank decreases, which slows down the rate of hydrogen desorption reaction. This property makes the solid-state hydrogen storage technique safer than the compressed hydrogen storage technique and liquid hydrogen storage technique.

Remark 1. Here charge refers to the process of hydrogen entering the internal space of the MH tank from the pipe while absorption refers to the process of hydrogen reacting with metal alloy. Charging only depends on the pressure difference between the pipe pressure and the tank pressure while absorption only depends on the pressure difference between the tank pressure and the absorption equilibrium pressure. The difference between discharging and desorption is similar.

3. TWO-DIMENSIONAL STATE-SPACE MODEL

We first consider the physical model of the MH tank. Several assumptions widely used in the modeling of MH tanks are listed to simplify the modeling process (Busqué et al. (2018), Keow et al. (2021)):

(1) The heat transfer coefficient of the MH tank shell is sufficiently large.
(2) The gas satisfies the ideal gas law.
(3) Neglect the change of MH volume during absorption and desorption.

Considering the mass balance of gaseous hydrogen in the MH tank one can get:

$$\frac{\mathrm{d}\rho_\mathrm{g}}{\mathrm{dt}} = \frac{m'_{in} - m'_r}{V_{tank} - V_{MH} + V_{MH}\cdot\varepsilon}, \tag{2}$$

where ρ_g is the density of hydrogen, m'_{in}(kg/s) is the mass flow rate of hydrogen (charge:+, discharge:-), m'_r(kg/s) is the sorption mass flow rate of hydrogen (absorption:+, desorption:-), V_{tank} and V_{MH} are the volumes of the tank and the MH, respectively, ε is the porosity of the MH. The numerator of the right term represents the change in mass of gaseous hydrogen in the MH tank per unit time, while the denominator represents the volume of gaseous hydrogen in the MH tank. Equation (2) can be normalized by V_{MH} and it can be rewritten that

$$\frac{\mathrm{d}\rho_{\mathrm{g}}}{\mathrm{dt}} = \frac{f_{in} - f_r}{V_g}, \tag{3}$$

where

$$f_{in} \triangleq \frac{m'_{in}}{V_{MH}} \tag{4}$$

is the normalized mass flow rate of hydrogen,

$$f_r \triangleq \frac{m'_r}{V_{MH}} \tag{5}$$

is the normalized sorption mass flow rate of hydrogen, and

$$V_g \triangleq \frac{V_{tank}}{V_{MH}} - 1 + \varepsilon \tag{6}$$

is the normalized volume of hydrogen.

Considering the mass balance of the MH:

$$\frac{\mathrm{d}\rho_{\mathrm{s}}}{\mathrm{dt}} = \frac{m'_r}{V_{MH} - V_{MH} \cdot \varepsilon}, \tag{7}$$

where ρ_s is the density of the MH. The numerator of the right term represents the change in mass of the MH per unit time, while the denominator represents the volume of the MH. Similarly, (7) can be rewritten as

$$\frac{\mathrm{d}\rho_{\mathrm{s}}}{\mathrm{dt}} = \frac{f_r}{V_s}, \tag{8}$$

where

$$V_s \triangleq 1 - \varepsilon \tag{9}$$

is the normalized volume of the MH.

The calculation of the normalized mass flow rate f_{in} based on pressure is a challenge. Gehring et al. (2024) utilize the polytropic and reversible adiabatic outflow equation of an ideal gas to calculate the mass flow rate into the tank. To decrease the computation cost, a simple pipe model is used in this work:

$$f_{in} = k_p \cdot P_{dif} \cdot 10^{-5}, \tag{10}$$

where k_p is the proportional coefficient, and

$$P_{dif} \triangleq P_{pipe} - P \tag{11}$$

is the pressure difference between the pipe pressure and tank pressure.

Remark 2. In (10), we use a proportion model to calculate the normalized mass flow rate f_{in}. Using a polynomial on the pressure difference P_{dif} may give a better fit to the actual mass flow rate, but it also increases the number of unknown parameters.

Tank pressure can be calculated based on the ideal gas law:

$$P = \rho_g \frac{TR}{M_{H_2}}, \tag{12}$$

where M_{H_2} is the molar mass of hydrogen, T is the temperature of the MH tank which can be measured by the thermocouple and R is the universal gas constant. The normalized sorption mass flow rate of hydrogen f_r can be expressed as (Jemni and Nasrallah (1995a,b)):

$$f_r = \begin{cases} C_a e^{-\frac{E_a}{RT}} \ln\left(\dfrac{P}{P_{eq,a}}\right)(\rho_{ss} - \rho_s), P > P_{eq,a} \\ C_d e^{-\frac{E_d}{RT}} \left(\dfrac{P - P_{eq,d}}{P_{eq,d}}\right)(\rho_s - \rho_{s0}), P < P_{eq,d} \\ 0, \text{otherwise} \end{cases}$$

where C_a and C_d are the absorption and desorption constants, E_a and E_d are the activation energy for absorption and desorption, $P_{eq,a}$ and $P_{eq,d}$ are the equilibrium pressure for absorption and desorption, respectively. ρ_{ss} is the saturated density of the MH with complete absorption of hydrogen and ρ_{s0} is the empty density of the MH without any hydrogen. Equilibrium pressures can be expressed as (Gonzatti et al. (2018)):

$$\ln\frac{P_{eq,a}}{P_0} = \frac{\Delta S_d}{R} - \frac{\Delta H_d}{RT} + (\varphi + \varphi_0)\tan\left[\pi\left(\frac{\rho_s - \rho_{s0}}{\rho_{ss} - \rho_{s0}} - 0.5\right)\right] + \frac{\beta}{2}, \tag{14}$$

$$\ln\frac{P_{eq,d}}{P_0} = \frac{\Delta S_d}{R} - \frac{\Delta H_d}{RT} + (\varphi - \varphi_0)\tan\left[\pi\left(\frac{\rho_s - \rho_{s0}}{\rho_{ss} - \rho_{s0}} - 0.5\right)\right] - \frac{\beta}{2}, \tag{15}$$

where ΔH_d is the enthalpy change for desorption, ΔS_d is the entropy change for desorption, P_0 is the atmospheric pressure, φ and φ_0 are the plateau flatness coefficients and β is the plateau hysteresis coefficient.

Based on the above deduction, the two-dimensional state-space model for the MH tank can be finally obtained:

$$\dot{\mathbf{x}} = \begin{bmatrix} \dfrac{k_p \cdot (u_2 - \dfrac{x_1 u_1 R}{M_{H_2}}) \cdot 10^{-5} - f_r}{V_g} \\ \dfrac{f_r}{V_s} \end{bmatrix}, \tag{16}$$

$$y = k_p \cdot (u_2 - \frac{x_1 u_1 R}{M_{H_2}}) \cdot 10^{-5}, \tag{17}$$

where

$$\mathbf{x} = \begin{bmatrix} x_1 \\ x_2 \end{bmatrix} = \begin{bmatrix} \rho_g \\ \rho_s \end{bmatrix}, \mathbf{u} = \begin{bmatrix} u_1 \\ u_2 \end{bmatrix} = \begin{bmatrix} T \\ P_{pipe} \end{bmatrix}, y = f_{in} \tag{18}$$

are the states, inputs and output of the system, respectively.

4. PARAMETER SENSITIVITY ANALYSIS

The First-order Trajectory Sensitivity Analysis (FOTSA) method (Kong et al. (2015)) can effectively analyze the sensitivity of parameters in nonlinear systems.

For a given system:

$$\dot{\mathbf{x}} = \mathbf{f}(\mathbf{x}, \mathbf{u}, \boldsymbol{\theta}), \tag{19}$$

$$\mathbf{y} = \mathbf{h}(\mathbf{x}, \mathbf{u}, \boldsymbol{\theta}), \tag{20}$$

where $\mathbf{x} \in \mathbb{R}^n$ denotes the state vector; $\mathbf{u} \in \mathbb{R}^m$ is the input vector; $\boldsymbol{\theta} \in \mathbb{R}^p$ is a constant parameter vector; $\mathbf{f} \in \mathbb{R}^n$ is the vector field and $\mathbf{h} \in \mathbb{R}^l$ is the output function.

For the dynamic system defined by (19) and (20), we define $\mathcal{X}(t, t_0, \mathbf{x}_{t_0}, \mathbf{u}, \boldsymbol{\theta})$ as the trajectory of the solution which depends on the interval $t \in [t_0, t_d]$, the initial state $\mathbf{x}_{t_0} \triangleq \mathbf{x}(t_0)$, the system inputs $\mathbf{u}$ and the parameters $\boldsymbol{\theta}$. For the sake of simplicity, define $\mathcal{X} \triangleq \mathcal{X}(t, t_0, \mathbf{x}_{t_0}, \mathbf{u}, \boldsymbol{\theta})$ and $\dot{\mathcal{X}} \triangleq \frac{\partial \mathcal{X}(t, t_0, \mathbf{x}_{t_0}, \mathbf{u}, \boldsymbol{\theta})}{\partial t}$.

To investigate the variations in system states caused by the variations in the system unknown parameters $\Delta\boldsymbol{\theta}$, the first-order Taylor expansion of (19) is expressed as follows:

$$\mathcal{X}(\boldsymbol{\theta} + \Delta\boldsymbol{\theta}) = \mathcal{X}(\boldsymbol{\theta}) + \left(\frac{\partial \mathcal{X}(\boldsymbol{\theta})}{\partial \boldsymbol{\theta}}\right) \cdot \Delta\boldsymbol{\theta} + o(\boldsymbol{\theta}). \tag{21}$$

Defining the changes in the trajectory of the system solution $\Delta\mathcal{X} \triangleq \mathcal{X}(\boldsymbol{\theta}+\Delta\boldsymbol{\theta}) - \mathcal{X}(\boldsymbol{\theta})$, (21) can be rewritten as

$$\Delta\mathcal{X} = \left(\frac{\partial\mathcal{X}(\boldsymbol{\theta})}{\partial\boldsymbol{\theta}}\right)\cdot\Delta\boldsymbol{\theta} + o(\boldsymbol{\theta}), \tag{22}$$

where $o(\boldsymbol{\theta})$ is the Taylor residual. If the term $\partial\mathcal{X}(\boldsymbol{\theta})/\partial\boldsymbol{\theta}$ can be computed, then the relationship between state variation $\Delta\mathcal{X}$ caused by parameter variation $\Delta\boldsymbol{\theta}$ is obtained.

Therefore, we compute the sensitivity of the derivative of the solution as

$$\frac{\partial\dot{\mathcal{X}}}{\partial\boldsymbol{\theta}} = \frac{\partial\mathbf{f}}{\partial\mathcal{X}}\cdot\frac{\partial\mathcal{X}}{\partial\boldsymbol{\theta}} + \frac{\partial\mathbf{f}}{\partial\mathbf{u}}\cdot\frac{\partial\mathbf{u}}{\partial\boldsymbol{\theta}} + \frac{\partial\mathbf{f}}{\partial\boldsymbol{\theta}}. \tag{23}$$

Assuming the system input $\mathbf{u}$ is independent of the system unknown parameters $\boldsymbol{\theta}$, then

$$\frac{\partial\mathbf{u}}{\partial\boldsymbol{\theta}} = \mathbf{0} \in \mathbb{R}^{m\times p}. \tag{24}$$

Consequently, (23) can be simplified to

$$\frac{\partial\dot{\mathcal{X}}}{\partial\boldsymbol{\theta}} = \frac{\partial\mathbf{f}}{\partial\mathcal{X}}\cdot\frac{\partial\mathcal{X}}{\partial\boldsymbol{\theta}} + \frac{\partial\mathbf{f}}{\partial\boldsymbol{\theta}}. \tag{25}$$

Note that $\frac{\partial\frac{\partial\mathcal{X}}{\partial t}}{\partial\boldsymbol{\theta}} = \frac{\partial\frac{\partial\mathcal{X}}{\partial\boldsymbol{\theta}}}{\partial t}$ and define FOTSF as

$$\boldsymbol{\lambda} \triangleq \frac{\partial\mathcal{X}}{\partial\boldsymbol{\theta}} \in \mathbb{R}^{n\times p}, \tag{26}$$

then (25) is rewritten as

$$\dot{\boldsymbol{\lambda}} = \frac{\partial\mathbf{f}}{\partial\mathbf{x}}\boldsymbol{\lambda} + \frac{\partial\mathbf{f}}{\partial\boldsymbol{\theta}}. \tag{27}$$

We assume the initial value of FOTSF is independent of $\boldsymbol{\theta}$. Consequently $\boldsymbol{\lambda}(t_0) = \mathbf{0}$.

Substituting (26) into (21), we can get

$$\Delta\mathcal{X} = \boldsymbol{\lambda}\cdot\Delta\boldsymbol{\theta} + o(\boldsymbol{\theta}). \tag{28}$$

The solution of $\boldsymbol{\lambda}$ can be obtained by solving (27), which shows the effect on the state of the system, $\mathbf{x}$, caused by the variations in the unknown parameters $\boldsymbol{\theta}$.

Each state variation caused by a single parameter variation is

$$\Delta\mathcal{X}_i = \lambda_{i,j}\cdot\Delta\theta_j + o(\theta), \tag{29}$$

where $i = 1, 2$ is the component of the states and $j = 1, 2\cdots p$ is the component of sensitivity and parameters.

The maximum absolute value of each $\Delta\mathcal{X}_i$ under the same percentage of each parameter $\Delta\theta_j$ during $t \in [t_0, t_d]$ is chosen as the sensitivity index s_i, which can be expressed as:

$$s_i = \max|\Delta\mathcal{X}_i|. \tag{30}$$

For all unknown parameters, one can calculate the corresponding sensitivity index. The parameter with a higher sensitivity index has a greater impact on the trajectory of the system state while the parameter with a lower sensitivity index has a smaller impact.

We check the sensitivity of the following unknown parameters in the two-dimensional model: $\boldsymbol{\theta_s} = [\Delta S_d, \Delta H_d, \varphi, \varphi_0, \beta, C_a, C_d, E_a, E_d] \subset \boldsymbol{\theta}$.

An operating profile which includes the charging and discharging process is defined to analyze the sensitivity. In the model (16) (17), temperature is considered a measurable variable. To calculate the sensitivity index of the parameters in numerical simulations, the temperature dynamics model needs to be used to generate the temperature data. The temperature of the MH tank can be calculated as (Nasrallah and Jemni (1997)):

$$\dot{T} = \frac{f_r\frac{\Delta H}{M_{H_2}} + f_r T(C_{pg} - C_{ps}) + Q}{V_g C_{pg}\rho_g + V_s C_{ps}\rho_s}, \tag{31}$$

where C_{pg} and C_{ps} are the specific heat of hydrogen and the MH, respectively.

The heat exchange per unit volume Q from the ambient air to the MH tank can be simplified by

$$Q = \frac{k_{amb}\cdot(T_{amb} - T)}{V_{MH}}, \tag{32}$$

where k_{amb} is the overall heat exchange coefficient between the ambient air and the MH tank, and T_{amb} is the ambient temperature.

To compute the coefficient items matrix $(\partial\mathbf{f}/\partial\mathcal{X})$, free items matrix $(\partial\mathbf{f}/\partial\boldsymbol{\theta_u})$ and further calculate the sensitivity index s_i in numerical simulations, nominal values of $\boldsymbol{\theta_s}$ need to be determined in advance. Nominal values can be chosen based on a reasonable range of reference values that have appeared in the literature (Kölbig et al. (2019); Barale et al. (2023); Capurso et al. (2016)). Table 1 and Table 2 list the nominal values and other parameters used in numerical simulations.

Table 1. FOTSF nominal values of parameters (Chen et al. (2024))

Parameter	Symbol	Nominal value
Entropy change for desorption	ΔS_d	111.77 J/mol/K
Enthalpy change for desorption	ΔH_d	2.668×10^4 J/mol
Plateau flatness coefficient	φ	0.1843
Plateau flatness coefficient	φ_0	0.0042
Plateau hysteresis coefficient	β	0.2355
Absorption constant	C_a	3928.1 1/s
Desorption constant	C_d	4952.2 1/s
Activation energy for absorption	E_a	3.8236×10^4 J/mol
Activation energy for desorption	E_d	3.0915×10^4 J/mol

Table 2. Other parameters used in the model (Keow et al. (2021))

Symbol	Value	Symbol	Value
ϵ	0.6997	V_{MH}	0.353×10^{-3} m^3
ρ_{s0}	6211.1 kg/m^3	ρ_{H_2}	0.0897 kg/m^3
R	8.314 J/(mol K)	P_0	101 325 Pa
M_{H_2}	2.016×10^{-3} kg/mol	T_{amb}	298.15 K
V_{tank}	0.48×10^{-3} m^3	k_p	0.06 s/m
V_{H_2}	0.35 m^3	k_{amb}	0.7 J/(s · K)
C_{pg}	14 890 J/(kg K)	C_{ps}	400 J/(kg K)

The initial conditions of operating profile are defined as $\rho_g(t_0)$=0.0813 kg/m^3 and $\rho_s(t_0)$ = 6217.5 kg/m^3. The operating profile is divided into three parts: The first part is the charging process. The initial pipe pressure is 0.1 MPa and pipe pressure increases by 0.2 MPa every 1500s until 2.1 MPa during $t \in [0, 15000s)$; In the second part, we keep the pipe pressure at 2.1 MPa during $t \in [15000s, 30000s)$. The third part is the discharging process and pipe pressure decreases by 0.15 MPa every 1500s until 0.6 MPa during

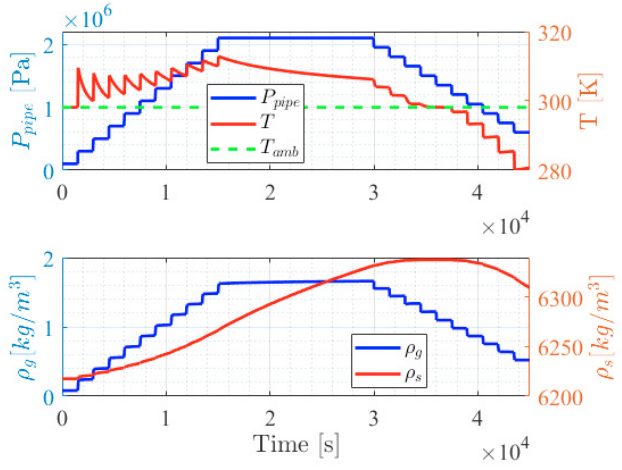

Fig. 2. The mixed charging & discharging profile of sensitivity analysis.

$t \in [30000s, 45000s)$; Figure 2 shows the system dynamics for the mixed charging & discharging process.

According to (27), the FOTSF $\lambda_{i,j}$ for ρ_g and ρ_s of each select parameter in the mixed charging & discharging process are shown in Figure 3 and Figure 4. We can observe that two parameters ΔS_d and ΔH_d have sustainable effects on the dynamic performance of the system state ρ_g and ρ_s. Three parameters φ, φ_0, β affect the state ρ_g at the beginning of the charging and discharging process but have sustainable effects on ρ_s. Parameters C_a and E_a affect the state ρ_g only during charge as the trajectories keep zero while C_d and E_d affect the state ρ_g only during discharge. The reason for zero trajectory is that the reaction kinetics f_r contain different parameters in the expressions for the charging and discharging processes. For instance, C_a and E_a only appear in the expression for charging, and when the system dynamics of the MH tank switches from charging to discharging, the system dynamics do not contain information about the constants C_a and E_a, and therefore the trajectory of these two parameters is always zero in discharging process. The trajectories of C_d and E_d have zero trajectories in the charging process for the same reason.

The sensitivity index for ρ_g and ρ_s are computed and listed in Table 3. Sensitivities for ρ_g, in descending order, are $\Delta S_d > \Delta H_d > E_a > \varphi > E_d > \beta$ and sensitivities for ρ_s, in descending order, are $\Delta S_d > \Delta H_d > \beta > \varphi > E_a > E_d$. Comparison results of sensitivity indicate that the six parameters ΔS_d, ΔH_d, φ, β, E_a and E_d have more impact on system states.

5. CONCLUSION

A two-dimensional model is proposed in this work, then the FOTSA method is used to analyze the sensitivity of unknown parameters. The results of the analysis show that in the process including charge and discharge, the minor variations of six parameters: entropy change for desorption ΔS_d, enthalpy change for desorption ΔH_d, activation energy for absorption E_a, activation energy for desorption E_d, plateau flatness coefficient φ and plateau hysteresis coefficient β cause larger state changes relative

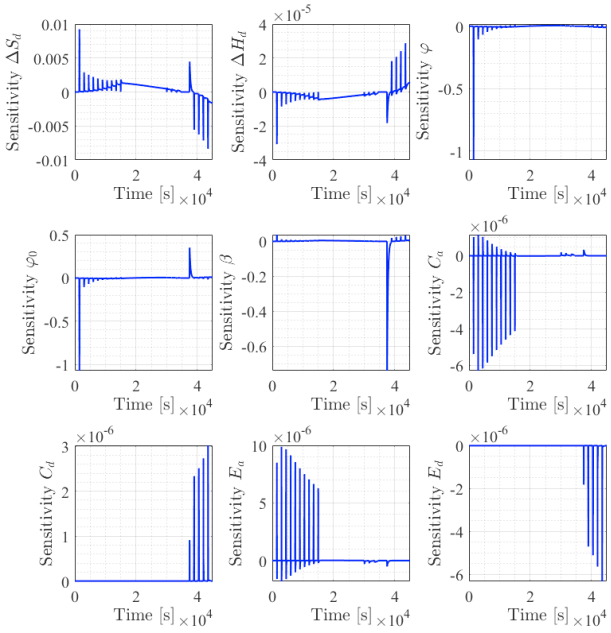

Fig. 3. Parameter sensitivity function for ρ_g of mixed charging & discharging process

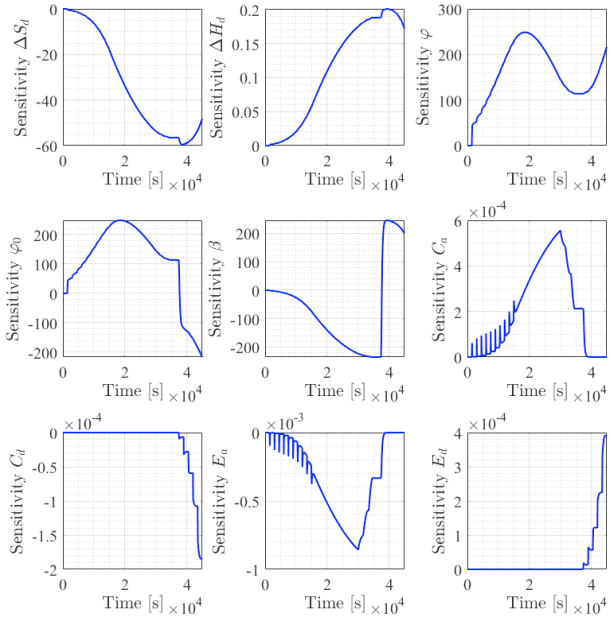

Fig. 4. Parameter sensitivity function for ρ_s of mixed charging & discharging process

to other parameters. The proposed model also can be used to estimate the unknown state ρ_s of the MH tank in a scenario where pipeline pressure is used as a control input and further used to estimate the SOC of the MH tank.

REFERENCES

Afzal, M., Mane, R., and Sharma, P. (2017). Heat transfer techniques in metal hydride hydrogen storage: A review. *International Journal of Hydrogen Energy*, 42(52), 30661–30682.

Barale, J., Nastro, F., Violi, D., Rizzi, P., Luetto, C., and Baricco, M. (2023). A metal hydride compressor for a

Table 3. Sensitivity index for ρ_g and ρ_s of mixed charging & discharging process with 10% parameter variation

Parameter	Symbol	$s_1(10\%)$	$s_2(10\%)$
Entropy change for desorption	ΔS_d	0.1033	665.1230
Enthalpy change for desorption	ΔH_d	0.0820	536.6964
Plateau flatness coefficient	φ	0.0197	4.5824
Plateau flatness coefficient	φ_0	$4.4943e-4$	0.1044
Plateau hysteresis coefficient	β	0.0174	5.7840
Absorption constant	C_a	0.0025	0.2181
Desorption constant	C_d	0.0015	0.0916
Activation energy for absorption	E_a	0.0378	3.2744
Activation energy for desorption	E_d	0.0195	1.2127

small scale h2 refuelling station. *International Journal of Hydrogen Energy*.

Benchluch, S.M. and Chow, J.H. (1993). A trajectory sensitivity method for the identification of nonlinear excitation system models. *IEEE Transactions on Energy Conversion*, 8(2), 159–164.

Busqué, R., Torres, R., Grau, J., Roda, V., and Husar, A. (2018). Mathematical modeling, numerical simulation and experimental comparison of the desorption process in a metal hydride hydrogen storage system. *International Journal of Hydrogen Energy*, 43(35), 16929–16940.

Capurso, G., Schiavo, B., Jepsen, J., Lozano, G., Metz, O., Saccone, A., De Negri, S., Bellosta von Colbe, J.M., Klassen, T., and Dornheim, M. (2016). Development of a modular room-temperature hydride storage system for vehicular applications. *Applied Physics A*, 122, 1–11.

Chen, M., Batlle, C., Escachx, B., Costa-Castelló, R., and Na, J. (2024). Sensitivity analysis and calibration for a two-dimensional state-space model of metal hydride storage tanks based on experimental data. *Journal of Energy Storage*, 94, 112316.

Choi, J., Harvey, J.W., and Conklin, M.H. (1999). Use of multi-parameter sensitivity analysis to determine relative importance of factors influencing natural attenuation of mining contaminants. In *Proceedings of the Toxic Substances Hydrology Program Meeting, Charleston, SC*, 185–192.

Christopher Frey, H. and Patil, S.R. (2002). Identification and review of sensitivity analysis methods. *Risk analysis*, 22(3), 553–578.

Correa, J.M., Farret, F.A., Popov, V.A., and Simoes, M.G. (2005). Sensitivity analysis of the modeling parameters used in simulation of proton exchange membrane fuel cells. *IEEE Transactions on Energy Conversion*, 20(1), 211–218.

Førde, T., Maehlen, J., Yartys, V., Lototsky, M., and Uchida, H. (2007). Influence of intrinsic hydrogenation/dehydrogenation kinetics on the dynamic behaviour of metal hydrides: A semi-empirical model and its verification. *International Journal of Hydrogen Energy*, 32(8), 1041–1049.

Gehring, D., Kölbig, M., Göltz, S., Heidingsfeld, J., Rentz, A., Sawodny, O., Linder, M., and Bürger, I. (2024). Metal hydride reactor for output temperature control. *International Journal of Hydrogen Energy*, 50, 1502–1517.

Gonzatti, F., Miotto, M., and Farret, F. (2018). Automation and analysis of the operation of (la0. 85ce0. 15) ni5 in energy storage plants. *International Journal of Hydrogen Energy*, 43(5), 2850–2860.

Hariyadi, A., Suwarno, S., Denys, R.V., von Colbe, J.B., Sætre, T.O., and Yartys, V. (2022). Modeling of the hydrogen sorption kinetics in an ab2 laves type metal hydride alloy. *Journal of Alloys and Compounds*, 893, 162135.

Jemni, A. and Nasrallah, S.B. (1995a). Study of two-dimensional heat and mass transfer during absorption in a metal-hydrogen reactor. *International Journal of Hydrogen Energy*, 20(1), 43–52.

Jemni, A. and Nasrallah, S.B. (1995b). Study of two-dimensional heat and mass transfer during desorption in a metal-hydrogen reactor. *International Journal of Hydrogen Energy*, 20(11), 881–891.

Keow, A.L.J., Mayhall, A., Cescon, M., and Chen, Z. (2021). Active disturbance rejection control of metal hydride hydrogen storage. *International Journal of Hydrogen Energy*, 46(1), 837–851.

Kölbig, M., Bürger, I., and Linder, M. (2019). Characterization of metal hydrides for thermal applications in vehicles below 0° c. *International Journal of Hydrogen Energy*, 44(10), 4878–4888.

Kong, X., Ba, K., Yu, B., Cao, Y., Wu, L., and Quan, L. (2015). Trajectory sensitivity analysis of first order and second order on position control system of highly integrated valve-controlled cylinder. *Journal of Mechanical Science and Technology*, 29, 4445–4464.

Nasrallah, S.B. and Jemni, A. (1997). Heat and mass transfer models in metal-hydrogen reactor. *International Journal of Hydrogen Energy*, 22(1), 67–76.

Nishizaki, T., Miyamoto, K., and Yoshida, K. (1983). Coefficients of performance of hydride heat pumps. *Journal of the Less Common Metals*, 89(2), 559–566.

Suárez, S.H., Chabane, D., N'Diaye, A., Ait-Amirat, Y., Elkedim, O., and Djerdir, A. (2022). Evaluation of the performance degradation of a metal hydride tank in a real fuel cell electric vehicle. *Energies*, 15(10), 3484.

Tarhan, C. and Çil, M.A. (2021). A study on hydrogen, the clean energy of the future: Hydrogen storage methods. *Journal of Energy Storage*, 40, 102676.

Xiao, J., Zeng, X., Chen, H., and Yang, L. (2023). An investigation into the multi-parameter identification and model optimization strategy of the pct curves of hydrogen storage alloys by multiple intelligent algorithms. *International Journal of Hydrogen Energy*, 48(5), 1943–1955.